

Crystal Graph Convolutional Neural Networks for Accurate and Interpretable Prediction of Material Properties

Tian Xie and Jeffrey C. Grossman

*Department of Materials Science and Engineering,
Massachusetts Institute of Technology, Cambridge, Massachusetts 02139, United States*

(Dated: March 1, 2022)

The use of machine learning methods for accelerating the design of crystalline materials usually requires manually constructed feature vectors or complex transformation of atom coordinates to input the crystal structure, which either constrains the model to certain crystal types or makes it difficult to provide chemical insights. Here, we develop a crystal graph convolutional neural network (CGCNN) framework to directly learn material properties from the connection of atoms in the crystal, providing a universal and interpretable representation of the crystals structure. Our method achieves the same accuracy as DFT for 8 different properties of crystals with various structure types and compositions after trained with 10^4 data points. Further, our framework is interpretable because one can extract the contributions from local chemical environments to global properties. Using an example of perovskites, we show how this information can be utilized to discover empirical rules for materials design.

Machine learning (ML) methods are becoming increasingly popular in accelerating the design of new materials by predicting material properties with accuracy close to *ab-initio* calculations, but with computational speeds orders of magnitude faster[1–3]. The arbitrary size of crystal systems poses a challenge as they need to be represented as a fixed length vector in order to be compatible with most ML algorithms. This problem is usually resolved by manually constructing fixed-length feature vectors using simple material properties[1, 3–5] or designing symmetry-invariant transformations of atom coordinates[6–8]. However, the former requires case-by-case design for predicting different properties and the latter makes it hard to interpret the models as a result of the complex transformations.

In this letter, we present a generalized crystal graph convolutional neural networks (CGCNN) framework for representing periodic crystal systems that provides both material property prediction with DFT accuracy and atomic level chemical insights. Recent advances in “deep learning” have enabled learning from a very raw representation of data, e.g. pixels of an image, making it possible to build general models that outperforms traditionally expert designed representations[9]. By looking into the simplest form of crystal representation, i.e. the connection of atoms in the crystal, we directly build convolutional neural networks (CNN) on top of crystal graphs generated from crystal structures. The CGCNN achieves similar accuracy with respect to DFT calculations as DFT compared with experimental data for eight different properties after being trained with data from the Materials Project[10], indicating the generality of this method. We also demonstrate the interpretability of CGCNN by extracting the energy of each site in the perovskite structure from the total energy, an example of learning the contribution of local chemical environments to the global property. The empirical rules generalized

from the results are consistent with the common knowledge for discovering more stable perovskites and can significantly reduce the search space for high throughput screening.

The main idea in our approach is to represent the crystal structure by a crystal graph (CG) that encodes both atomic information and bonding interactions between atoms, and then build a convolutional neural network (CNN) on top of the graph to automatically extract representations that are optimum for predicting target properties by training with DFT calculated data. As illustrated in Figure 1 (a), a crystal graph \mathcal{G} is an undirected multigraph which is defined by N nodes and M edges, where N is the number of atoms in the primitive cell and M is the number of connections between atoms (the method for determining atom connectivity is explained in Supplemental Material). The CG is unlike normal graphs since it allows multiple edges between the same pair of end nodes, a characteristic for crystal graphs due to its periodicity, in contrast to molecular graphs. Each node i is represented by a feature vector \mathbf{v}_i , encoding the property of the atom corresponding to node i . Similarly, each edge $(i, j)_k$ is represented by a feature vector $\mathbf{u}_{(i,j)_k}$ corresponding to the k -th bond connecting atom i and atom j .

The CNN built on top of the CG consists of two major components: convolutional layers and pooling layers. Similar architectures have been used for image classification[11], natural language processing[12], and molecular fingerprinting[13], but not for crystal property prediction to the best of our knowledge. The convolutional layers repeatedly update the atom feature vector \mathbf{v}_i by “convolution” with surrounding atoms and bonds,

$$\mathbf{v}_i^{(t+1)} = g \left[\left(\sum_{j,k} \mathbf{v}_j^{(t)} \oplus \mathbf{u}_{(i,j)_k} \right) \mathbf{W}_c^{(t)} + \mathbf{v}_i^{(t)} \mathbf{W}_s^{(t)} + \mathbf{b}^{(t)} \right] \quad (1)$$

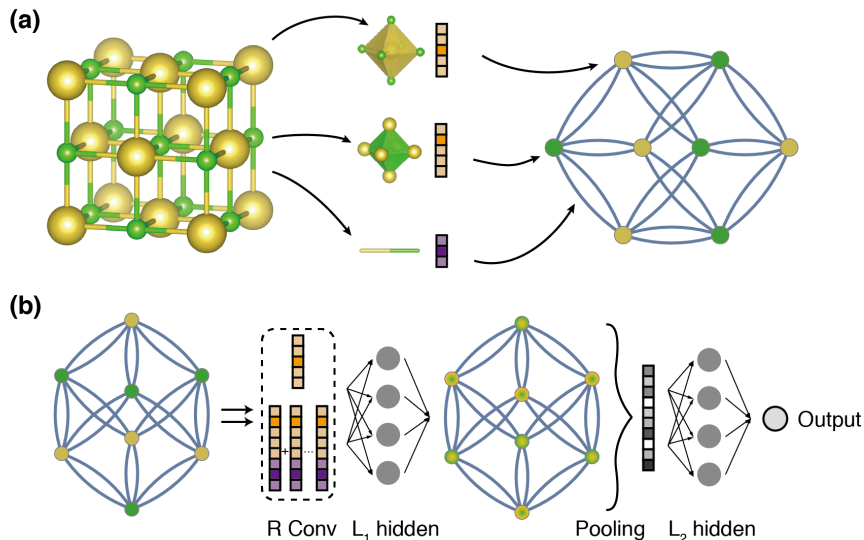


FIG. 1. Illustration of the crystal graph convolutional neural network (CGCNN). (a) Generation of the crystal graph. Crystals are converted to graphs with nodes representing atoms in the unit cell and edges representing atom connections. Nodes and edges are characterized by vectors corresponding to the atoms and bonds in the crystal, respectively. (b) Structure of the convolutional neural network on top of the crystal graph. R convolutional layers and L_1 hidden layers are built on top of each node, resulting in a new graph with each node representing the local environment of each atom. After pooling, a vector representing the entire crystal is connected to L_2 hidden layers, followed by the output layer to provide the prediction.

where \oplus denotes concatenation of atom and bond feature vectors, $\mathbf{W}_c^{(t)}$, $\mathbf{W}_s^{(t)}$, $\mathbf{b}^{(t)}$ are the convolution weight matrix, self weight matrix, and bias of the t -th layer, respectively, and g is the activation function for introducing non-linear coupling between layers. After R convolutions, the CNN automatically learns the feature vector $\mathbf{v}_i^{(R)}$ for each atom by iteratively including its surrounding environment. The pooling layer is then used for producing an overall feature vector \mathbf{v}_c for the crystal, which can be represented by a pooling function p ,

$$\mathbf{v}_c = p\left(\mathbf{v}_0^{(0)}, \mathbf{v}_1^{(0)}, \dots, \mathbf{v}_N^{(0)}, \dots, \mathbf{v}_N^{(R)}\right) \quad (2)$$

that satisfies permutational invariance with respect to atom indexing and size invariance with respect to unit cell choice. In this work, a normalized summation is used as the pooling function for simplicity but other functions can also be used. In addition to the convolutional and pooling layers, two fully-connected hidden layers with the depth of L_1 and L_2 are added to capture the complex mapping between crystal structure and property. Finally, an output layer is used to connect the L_2 hidden layer to predict the target property \hat{y} .

The training is performed by minimizing the difference between the predicted property \hat{y} and the DFT calculated property y , defined by a cost function $J(y, \hat{y})$. The whole CGCNN can be considered as a function f parameterized by \mathbf{W} that maps a crystal \mathcal{C} to the target property \hat{y} . Using backpropagation and stochastic gradient descent (SGD), we can solve the following optimization problem by iteratively updating the weights with DFT calculated

data,

$$\min_{\mathbf{W}} J(y, f(\mathcal{C}; \mathbf{W})) \quad (3)$$

the learned weights can then be used to predict material properties and provide chemical insights for future materials design.

In Supplemental Material (SM), we use a simple example to illustrate how a CGCNN composed of one linear convolution layer and one pooling layer can differentiate two crystal structures. With multiple convolution layers, pooling layers and hidden layers, CGCNN can extract any structure differences based on the atom connections and discover the underlying relations between structure and property.

To demonstrate the generality of the CGCNN, we train the model using calculated properties from the Materials Project[10]. We focus on two types of generality in this work: (1) The structure types and chemical compositions for which our model can be applied, and (2) the number of properties that our model can accurately predict.

The database we used includes a diverse set of inorganic crystals ranging from simple metals to complex minerals. After removing ill-converged crystals, the full database has 46744 materials covering 87 elements, 7 lattice systems and 216 space groups. As shown in Figure 2(a), the materials consist of as many as seven different elements, with 90% of them binary, ternary and quaternary compounds. The number of atoms in the primitive cell ranges from 1 to 200, and 90% of crystals have less than 60 atoms(Figure S2). Considering most of the

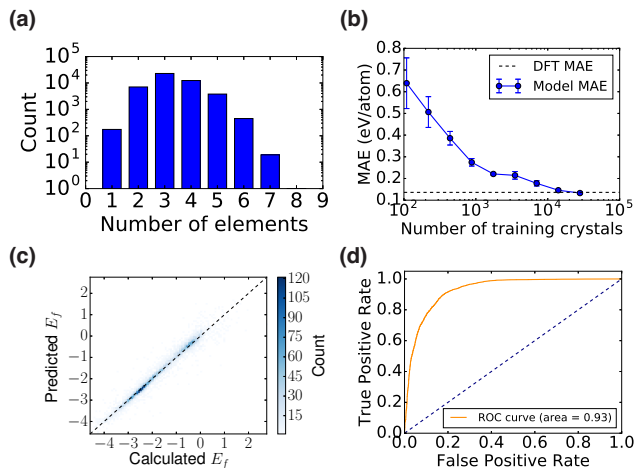


FIG. 2. The performance of CGCNN on the Materials Project database[10]. (a) Histogram representing the distribution of the number of elements in each crystal. (b) Mean absolute error (MAE) as a function of training crystals for predicting formation energy per atom. The dashed line denotes the MAE of DFT calculation compared with experiments[14]. (c) 2D histogram representing the predicted formation per atom against DFT calculated value. (d) Receiver operating characteristic (ROC) curve visualizing the result of metal-semiconductor classification. It plots the proportion of correctly identified semiconductors (true positive rate) against the proportion of correctly identified metals (false positive rate) under different thresholds.

crystals originate from the Inorganic Crystal Structure Database (ICSD)[15], this database is a good representative of known stoichiometric inorganic crystals.

We apply CGCNN to predict the formation energy of crystals in the database by a train-validation scheme. The CGCNN is a flexible framework that allows variance in the CG representation, CNN structure, and training process. For instance, the form of atom feature vector \mathbf{v}_i , the number of convolutional layers R , etc. can all be changed, resulting in different f in Eq. 3 and prediction performance. These hyperparameters are selected by training with 60% of the data and then validating with 20% to evaluate the performance. (Further detail can be found in Supplemental Material, including a list of optimized hyperparameters as shown in Table S1.) It is worth noting that a wide range of different hyperparameters gives prediction performance close to the optimum hyperparameters (Figure S3), indicating that the computation needed for hyperparameter optimization is relatively low. More interestingly, Figure S3(a) shows that using only group number and period number in the atom feature vector performs just slightly less accurately than using 10 different properties, suggesting that our model generalizes better than other methods that uses tens of atom properties[8, 16]. After selecting the optimum hyperparameters, the model is tested with the remaining 20% of data which are completely new to the model.

TABLE I. Summary of the prediction performance of seven different properties on test sets.

Property	# train data	Unit	MAE _{model}	MAE _{DFT}
Formation energy	28046	eV/atom	0.112	0.136[14]
Absolute energy	28046	eV/atom	0.227	0.19[17]
Band gap	16458	eV	0.530	0.6[17]
Fermi energy	28046	eV	0.564	–
Bulk moduli	2041	GPa	16.4	10.6[18]
Shear moduli	2041	GPa	13.4	6.86[18]
Poisson ratio	2041	–	0.033	–

Figure 2(b)(c) shows the performance of CGCNN on 9350 test crystals for predicting the formation energy per atom. As expected, we find a systematic decrease of the mean absolute error (MAE) of the predicted values compared with DFT calculated values as the number of training data is increased. The MAE first decreases linearly in the log scale plot, and then levels off as it approaches the MAE of DFT calculations with respect to experiments. This may be attributed to the random errors introduced during the DFT calculations, making it impossible to achieve accuracy below the DFT MAE[2]. Due to the diversity of crystal types and compositions in the database, roughly 10^4 crystals are needed to sample various possibilities of combining atoms to crystals in order to achieve the DFT accuracy. The best MAE we achieved is 0.112 eV/atom, lower than the estimated DFT accuracy of 0.136 eV/atom from the Open Quantum Materials Database (OQMD)[14]. The 2D histogram in Figure 2(c) shows that more than 90% of the crystals are predicted within 0.3 eV/atom error.

After establishing the generality of CGCNN with respect to the diversity of crystals, we next explore its prediction performance for different material properties. We apply the same framework to predict the absolute energy, band gap, Fermi energy, bulk moduli, shear moduli, and Poisson ratio of crystals using DFT calculated data from the Materials Project[10]. The same hyperparameter optimization method is applied although our results also show that there exists a set of hyperparameters can be used to achieve a MAE close to the optimum value for all properties (Table S4). We summarize the prediction performances in Table I and the corresponding 2D histograms in Figure S4. As we can see, the MAE of our model are close to or higher than DFT accuracy for most for properties when more than 10^4 training data is used. For elastic properties, the errors are higher since less data is available, and the DFT accuracy can be expected if more calculations can be done to sample the crystal space. For instance, as shown in Figure S5, by plotting the MAE as a function of the number of training crystals, we can infer that the DFT accuracy will be achieved when training size is around 10^4 .

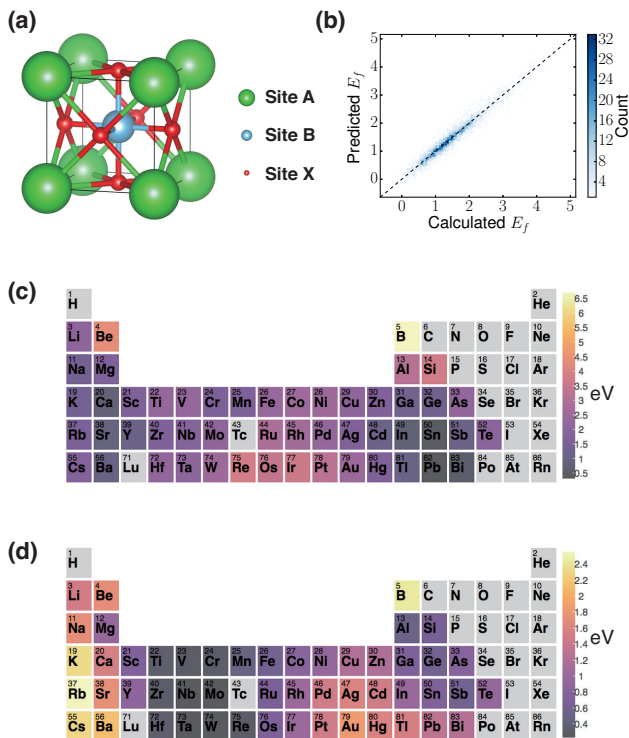


FIG. 3. Extraction of site energy of perovskites from total formation energy. (a) Structure of perovskites. (b) 2D histogram representing the predicted total formation against DFT calculated value. (c, d) Periodic table with the color of each element representing the mean of the site energy when the element occupies A site (c) or B site (d).

In addition to predicting continuous properties, CGCNN can also predict discrete properties by changing the output layer. By using a sigmoid activation function for the output layer and a cross entropy cost function, we can predict the classification of metal and semiconductor with the same framework. After hyperparameter optimization, in Figure 2(d), we show the receiver operating characteristic (ROC) curve of the prediction on 9350 test crystals. Excellent prediction performance is achieved with the area under the curve (AUC) at 0.93. By choosing a threshold of 0.5, we get metal prediction accuracy at 0.82, semiconductor prediction accuracy at 0.90, and overall prediction accuracy at 0.88.

Model interpretability is a desired property for any ML algorithms applied in materials science, because it can provide additional information for material design which may be more valuable than simply screening a large number of materials. However, non-linear functions are needed to learn the complex structure-property relations, resulting in ML models that are hard to interpret. CGCNN resolves this dilemma by separating the convolution and pooling layers. By using complex convolutions that include R convolutional and L_1 hidden layers but a linear pooling that includes one pooling layer that sums

and normalizes the last atom feature vector $\mathbf{v}_i^{(R)}$ and no L_2 hidden layers (details discussed in SM), we can learn the contribution of different local chemical environments, represented by $\mathbf{v}_i^{(R)}$ for each atom, to the target property while maintaining a model with high capacity to ensure the prediction performance.

We demonstrate how these local chemical environment related information can be used to provide chemical insights and guide the material design by a specific example: learning the energy of each site in perovskites from the total formation energy data. Perovskite is a crystal structure type with the form of ABX_3 , where the site A atom sits at a corner position, the site B atom sits at a body centered position and site X atoms sit at face centered positions (Figure 3(a)). The database[19] we use includes the formation energy of 18928 perovskite crystals, in which A and B sites can be any non-radioactive metals and X sites can be one or several elements from O, N, S, and F. We use the CGCNN with a linear pooling to predict the total formation energy of perovskites in the database, following a similar hyperparameter optimization procedure as for predicting other properties. The resulting MAE on 3787 test perovskites is 0.130 eV/atom as shown in Figure 3(b), which is slightly higher than using a complete pooling layer and L_2 hidden layers (0.099 eV/atom as shown in Figure S6) due to the additional constraints introduced by the simplified pooling layer. However, this CGCNN allows us to learn the energy of each site in the crystal while training with the total formation energy, providing additional insights for material design. Also, the prediction performance is still good considering the MAE of DFT calculated formation energies with respect to experimental values being 0.136 eV/atom for general crystals[14].

Figure 3(c, d) visualizes the mean of the predicted site energies when each element occupies the A and B site respectively. The most stable elements that occupy the A site are those with large radii due to the space needed for 12 coordinations. In contrast, elements with small radii like Be, B, Si are the most unstable for occupying the A site. For the B site, elements in groups 4, 5, and 6 are the most stable throughout the periodic table. This can be explained by crystal field theory, since the configuration of d electrons of these elements favors the octahedral coordination in the B site. Interestingly, the visualization shows that large atoms from groups 13-15 are stable in the A site, in addition to the well-known region of groups 1-3 elements. Inspired by this result, we applied a combinational search for stable perovskites using elements from group 13-15 as the A site and group 4-6 as the B site. We discovered 33 stable perovskites (Table S5) out of 378 where many of the compounds like $PbTiO_3$ [20], $PbZrO_3$ [20], and $SnTaO_3$ [21] have been experimentally synthesized. In general, chemical insights gained from CGCNN can significantly reduce the crystal space for high throughput screening. In comparison,

there are only 228 stable perovskites out of 18928 in our database: the chemical insight increased the search efficiency by a factor of 7.

In summary, we have developed a framework for representing crystal structures with arbitrary size and composition for machine learning tasks based on convolutional neural networks on top of crystal graphs. The model directly learns material properties from the connection of atoms in the crystal—a raw and thus universal representation of the crystal structure. The performance and generality of the model is tested through the prediction of seven continuous properties and one discrete property on a database composed of inorganic crystals with diverse structure types and compositions. We discover that DFT accuracy can be achieved for most properties when the training data size is around 10^4 , showing good generality on both the target property space and crystal space. Finally, we illustrate the interpretability of the framework by extracting the site energy of perovskites from the total formation energy. The chemical insights gained are consistent with common knowledge but also allows us to discover new regions of A site stability. The new knowledge gained from the CGCNN can significantly reduce the search space for high throughput screening.

This work was supported by Toyota Research Institute (TRI). Computational support was provided through the National Energy Research Scientific Computing Center, a DOE Office of Science User Facility supported by the Office of Science of the U.S. Department of Energy under Contract No. DE-AC02-05CH11231.

-
- [1] A. Seko, A. Togo, H. Hayashi, K. Tsuda, L. Chaput, and I. Tanaka, *Physical review letters* **115**, 205901 (2015).
- [2] F. A. Faber, A. Lindmaa, O. A. von Lilienfeld, and R. Armiento, *Physical Review Letters* **117**, 135502 (2016).
- [3] D. Xue, P. V. Balachandran, J. Hogden, J. Theiler, D. Xue, and T. Lookman, *Nature communications* **7** (2016).
- [4] L. M. Ghiringhelli, J. Vybiral, S. V. Levchenko, C. Draxl, and M. Scheffler, *Physical review letters* **114**, 105503 (2015).
- [5] O. Isayev, D. Fourches, E. N. Muratov, C. Oses, K. Rasch, A. Tropsha, and S. Curtarolo, *Chemistry of Materials* **27**, 735 (2015).
- [6] K. Schütt, H. Glawe, F. Brockherde, A. Sanna, K. Müller, and E. Gross, *Physical Review B* **89**, 205118 (2014).
- [7] F. Faber, A. Lindmaa, O. A. von Lilienfeld, and R. Armiento, *International Journal of Quantum Chemistry* **115**, 1094 (2015).
- [8] A. Seko, H. Hayashi, K. Nakayama, A. Takahashi, and I. Tanaka, *Physical Review B* **95**, 144110 (2017).
- [9] Y. LeCun, Y. Bengio, and G. Hinton, *Nature* **521**, 436 (2015).
- [10] A. Jain, S. P. Ong, G. Hautier, W. Chen, W. D. Richards, S. Dacek, S. Cholia, D. Gunter, D. Skinner, G. Ceder, *et al.*, *Apl Materials* **1**, 011002 (2013).
- [11] A. Krizhevsky, I. Sutskever, and G. E. Hinton, in *Advances in neural information processing systems* (2012) pp. 1097–1105.
- [12] R. Collobert and J. Weston, in *Proceedings of the 25th international conference on Machine learning (ACM, 2008)* pp. 160–167.
- [13] D. K. Duvenaud, D. Maclaurin, J. Iparraguirre, R. Bombarell, T. Hirzel, A. Aspuru-Guzik, and R. P. Adams, in *Advances in neural information processing systems* (2015) pp. 2224–2232.
- [14] S. Kirklin, J. E. Saal, B. Meredig, A. Thompson, J. W. Doak, M. Aykol, S. Rühl, and C. Wolverton, *npj Computational Materials* **1**, 15010 (2015).
- [15] M. Hellenbrandt, *Crystallography Reviews* **10**, 17 (2004).
- [16] O. Isayev, C. Oses, C. Toher, E. Gossett, S. Curtarolo, and A. Tropsha, *Nature Communications* **8** (2017).
- [17] A. Jain, G. Hautier, C. J. Moore, S. P. Ong, C. C. Fischer, T. Mueller, K. A. Persson, and G. Ceder, *Computational Materials Science* **50**, 2295 (2011).
- [18] M. De Jong, W. Chen, T. Angsten, A. Jain, R. Notestine, A. Gamst, M. Sluiter, C. K. Ande, S. Van Der Zwaag, J. J. Plata, *et al.*, *Scientific data* **2**, 150009 (2015).
- [19] I. E. Castelli, T. Olsen, S. Datta, D. D. Landis, S. Dahl, K. S. Thygesen, and K. W. Jacobsen, *Energy & Environmental Science* **5**, 5814 (2012).
- [20] G. Shirane, K. Suzuki, and A. Takeda, *Journal of the Physical Society of Japan* **7**, 12 (1952).
- [21] J. Lang, C. Li, X. Wang, *et al.*, *Materials Today: Proceedings* **3**, 424 (2016).